

Broadband and polarization-insensitive subwavelength grating reflector for the near-infrared region

Rui Zhang (张瑞), Yufei Wang (王宇飞), Yejin Zhang (张冶金), Zhigang Feng (冯志刚),
Fan Qi (祁帆), Lei Liu (刘磊), and Wanhua Zheng (郑婉华)*

State key Laboratory on Integrated Optoelectronics, Institute of Semiconductors,
Chinese Academy of Sciences, Beijing 100083, China

*Corresponding author: whzheng@semi.ac.cn

Received November 20, 2013; accepted December 31, 2013; posted online January 24, 2014

We propose a polarization-insensitive and broadband subwavelength grating reflector based on a multilayer structure. The reflector has an overlapped high reflectivity ($>99.5\%$) bandwidth of 248 nm between the TE and the TM polarizations, which is much higher than the previously reported results. We believe this subwavelength grating reflector can be applied to unpolarized devices.

OCIS codes: 050.1950, 050.5080, 050.6624, 230.4170.

doi: 10.3788/COL201412.020502.

Subwavelength gratings have attracted enormous attention theoretically and experimentally in the past few years^[1–5]. Due to the elimination of non-zero order diffraction according to the grating equation, subwavelength gratings are promising for many integrated optoelectronic applications such as polarizers^[1], couplers^[2], filters^[1,3], absorbers^[4], and reflectors^[5]. Besides, when surrounded by low-index material, they will demonstrate a high reflectivity over a broad wavelength range, which are so-called high-index-contrast subwavelength grating (HCG) reflectors^[5–8]. They can be applied to the vertical-cavity surface-emitting lasers (VCSELs) to replace the traditional distributed Bragg reflectors (DBRs) which are bulky and difficult to fabricate^[6–8]. Moreover, with a shortened cavity, HCG-VCSELs have many new properties, such as the single-mode operation and high-tuning speed^[8]. Additionally, with the progress of tunable VCSEL^[9], broadband property becomes more desirable. However, subwavelength gratings are polarization-selective inherently, thus they cannot be applied to light demultiplexing^[10], unpolarized lasers, or detectors.

Recently, Wu *et al.* reported a high performance polarization independent reflector based on a multilayered configuration grating structure^[11]. The reflector demonstrated a high reflection ($R > 99\%$) from 1.57 to 1.8 μm . However, the multi-subpart profile will bring considerable difficulties to the practical fabrication. We also demonstrated a polarization insensitive subwavelength grating reflector based on a semiconductor-insulator-metal structure. The reflector demonstrated an 89-nm overlapped high reflectivity ($> 99.5\%$) bandwidth^[5]. The mechanism of polarization-insensitivity was mainly attributed to the combined effect of HCG and metallic subwavelength grating with the insertion of insulator layer. However, the bandwidth can be further broadened by the redshift of the TM polarization reflectance spectra while increasing the reflectivity of both polarizations. In this letter, we propose a broadband and polarization-insensitive subwavelength grating reflector for the near-infrared region.

As shown in Fig. 1, the structure has a multilayered configuration, which is consisted of an $\text{Al}_{0.6}\text{Ga}_{0.4}\text{As}$

layer, a silica layer, an Au layer, a silica layer, and an Au layer from bottom to top, respectively. The refractive indexes for $\text{Al}_{0.6}\text{Ga}_{0.4}\text{As}$ and silica are 3.2 and 1.47, respectively. The Drude model^[12] is taken to depict the dispersion information of Au. The device is normally illuminated by a plane wave with both TE and TM polarized components, and is highly reflective in the zeroth order. The key parameters to be optimized are marked in Fig. 1, where the thicknesses of the layers from bottom to up, the period of subwavelength grating and the width of un-etched part are denoted as T_1 , T_2 , T_3 , T_4 , T_5 , A , and d , respectively. The rigorous coupled-wave analysis (RCWA)^[13,14] method is used to calculate the reflectance spectra.

Compared with the structure in Ref. [5], we insert a layer of silica grating and a layer of Au grating between the $\text{Al}_{0.6}\text{Ga}_{0.4}\text{As}$ grating layer and silica grating layer with the other parameters unchanged. By increasing the thickness of the silica grating layer, the wavelength of constructive interference^[15] for TM polarization light will become longer. The shifts of wavelength are represented by the shift of point 'A' in Fig. 2(a), which is at the bottom of TM polarization reflectance spectra. As to the TE polarization light, its wavelength shift will be represented by the shift of point 'B' in Fig. 2(a), which is at the bottom of the TE polarization reflectance spectra. The shifts of point 'A' and point 'B' with the increase of T_2 are demonstrated in Figs. 2(b) and (c), respectively. It can be seen that point 'B' moves slower than point 'A'. This can be explained by the relatively low reflectivity of

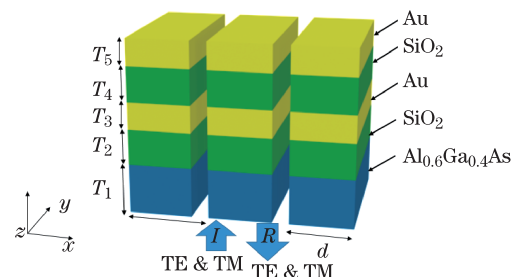


Fig. 1. Schematic configuration of our proposed structure.

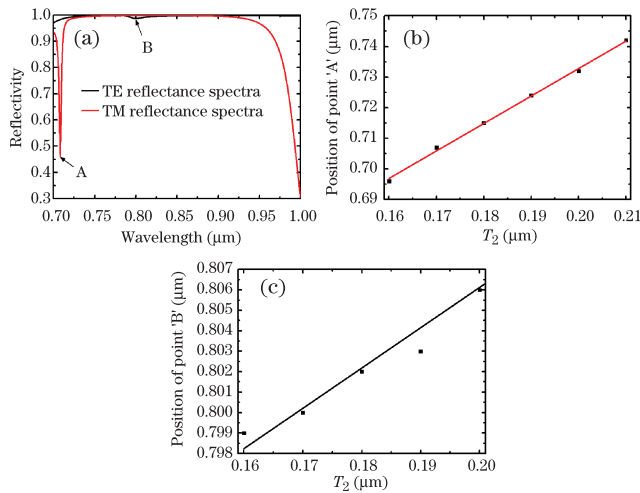


Fig. 2 (a) Reflectance spectra after inserting two layers. Positions of points (b) 'A' and (c) 'B' with the increase of T_2 .

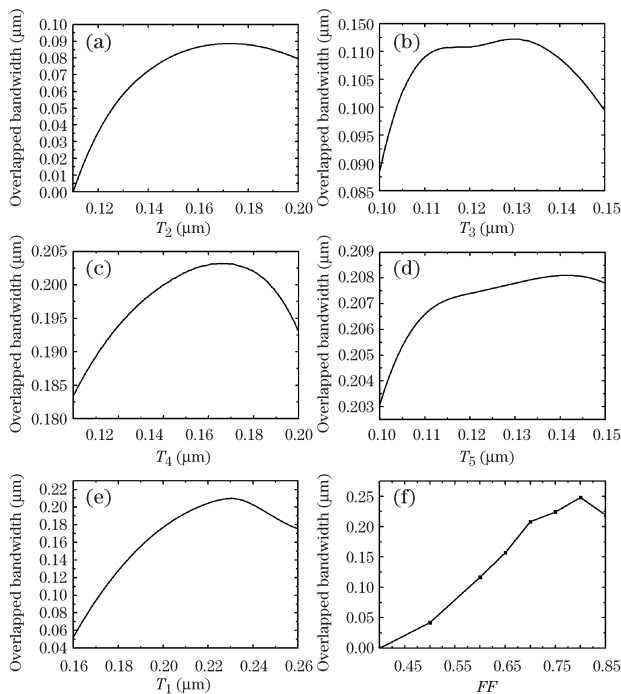


Fig. 3 Variation of overlapped bandwidth versus (a) the thickness of the first silica grating layer T_2 when $T_1=235$ nm, $T_3=100$ nm, $T_4=400$ nm, $T_5=100$ nm, $FF=0.7$; (b) the thickness of the first Au grating layer T_3 with T_2 already optimized; (c) the thickness of the second silica grating layer with T_2 and T_3 already optimized; (d) the thickness of second Au grating layer with T_2 , T_3 , and T_4 already optimized; (e) the thickness of $Al_{0.6}Ga_{0.4}As$ grating layer with T_2 , T_3 , T_4 , T_5 already optimized; (f) FF .

one-dimensional semiconductor material grating for TE polarization light^[16]. Besides, from the equation

$$2 \times n_{\text{eff}} \times \Delta T_2 = N \times \Delta \lambda, \quad (1)$$

where the refractive index of silica $n_{\text{eff}}=1.47$; $\Delta \lambda$ and ΔT_2 are the differences of λ and T_2 , respectively; N is an integer. The calculated slope ($\Delta \lambda / \Delta T_2$) is 0.98 when N is equal to 3. This value is very close to the result given by RCWA method, which is 0.89 after curve fitting. The

little difference between them can be explained that only part of the TM polarization light is involved in the interference.

We further scan and optimize the key parameters including T_1 , T_2 , T_3 , T_4 , T_5 , and FF defined by d/Λ . The period is kept unchanged. Additionally, the bandwidth presented in Fig. 3 is the result after multiplied by a proper constant to maximize the bandwidth within the range of $0.7-1 \mu\text{m}$ according to the scale effect of photonic crystals^[17]. For example, if the overlapped bandwidth is $0.8-1.1 \mu\text{m}$, then the dimensions of the reflector will be multiplied by $1/1.1$ with the other parameters unchanged. As a result, the overlapped bandwidth will shift to $0.727-1 \mu\text{m}$, within the range of $0.7-1 \mu\text{m}$.

The scanned results for T_1 , T_2 , T_3 , T_4 , T_5 , and FF are demonstrated in Fig. 3. When the biggest overlapped bandwidth is achieved, the optimal values for these parameters are $0.235 \mu\text{m}$, $0.170 \mu\text{m}$, $0.130 \mu\text{m}$, $0.170 \mu\text{m}$, $0.120 \mu\text{m}$, and 0.8 , respectively. And the overlapped bandwidth is $0.800-0.884$ and $0.902-1.081 \mu\text{m}$. After multiplying the dimensions of the reflector by $1/1.081$, the period, T_1 , T_2 , T_3 , T_4 , T_5 , and FF now are $0.352 \mu\text{m}$, $0.217 \mu\text{m}$, $0.157 \mu\text{m}$, $0.120 \mu\text{m}$, $0.157 \mu\text{m}$, $0.130 \mu\text{m}$, and 0.8 , respectively. The overlapped bandwidth are 248 nm, ranging from 0.740 to $0.818 \mu\text{m}$ and 0.834 to $1 \mu\text{m}$, as shown in Fig. 4. The absorptance spectra and transmittance spectra are also demonstrated in Fig. 4. It can be seen that although some absorption loss exists in the range of $0.7-1 \mu\text{m}$, the transmission loss is almost negligible. Besides, the absorption loss is below 0.5% in most wavelength region from 0.7 to $1 \mu\text{m}$.

In conclusion, we demonstrate a subwavelength grating reflector based on a multilayer configuration. Compared to the previous works, layers of silica grating and Au grating are inserted between the original $Al_{0.6}Ga_{0.4}As$ grating layer and silica grating layer. As a result, the overlapped bandwidth between the TE and TM polarization lights reaches 248 nm, which means the reflector is polarization-insensitive for the wavelength from 0.74 to $0.818 \mu\text{m}$ and from 0.834 to $1 \mu\text{m}$. We believe that this subwavelength grating reflector can replace the top DBR of single-mode unpolarized VCSEL, and can also be applied to other unpolarized devices.

This work was supported by the Chinese National Key Basic Research Special Fund (Nos. 2012CB933501 and 2011CB922002), the National Natural Science Foundation of China (Nos. 61025025, 61274070, 61021003,

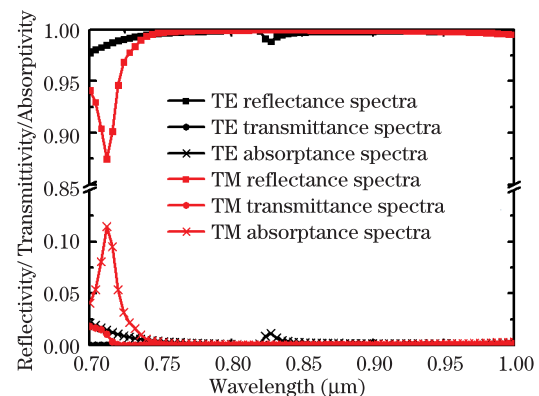


Fig. 4. Simulation results of our structure.

61234004, 61205043, 61137003, and 60838003), and the National “863” Program of China (Nos. 2012AA012202 and 2013AA030501).

References

1. Y. F. Xue, C. H. Wang, G. J. Zhang, and B. Cao, *Opt. Commun.* **284**, 501 (2011).
2. X. C. Xu, H. Subbaraman, J. Covey, D. Kwong, A. Hosseini, and R. T. Chen, *Appl. Phys. Lett.* **101**, 031109 (2012).
3. H. Honma, K. Takahashi, M. Ishida, and K. Sawada, *Jpn. J. Appl. Phys.* **51**, 11PA01 (2012).
4. D. L. Brundrett, T. K. Gaylord, and E. N. Glytsis, *Appl. Opt.* **37**, 2534 (1998).
5. A. J. Liu, F. Y. Fu, Y. F. Wang, B. Jiang, and W. H. Zheng, *Opt. Express* **20**, 14991 (2012).
6. T. Ansbaek, I. S. Chung, E. S. Semenova, and K. Yvind, *IEEE Photon. Technol. Lett.* **25**, 365 (2013).
7. M. C. Y. Huang, Y. Zhou, and C. J. Chang-Hasnain, *Nat. Photon.* **1**, 119 (2007).
8. I. S. Chung, V. Iakovlev, A. Sirbu, A. Mereuta, A. Caliman, E. Kapon, and J. Mork, *IEEE J. Quantum Electron.* **25**, 2297 (1989).
9. Y. Zhou, M. C. Y. Huang, C. Chase, V. Karagodsky, M. Moewe, B. Pesela, F. G. Sedgwick, and C. J. Chang-Hasnain, *IEEE J. Sel. Top. Quantum* **15**, 1485 (2009).
10. E. Popov, J. Hoose, B. Frankel, C. Keast, M. Fritze, T. Y. Fan, D. Yost, and S. Rabe, *Opt. Express* **12**, 269 (2004).
11. H. M. Wu, W. Q. Mo, J. Hou, D. S. Gao, R. Hao, H. Jiang, R. M. Guo, W. H. Wu, and Z. P. Zhou, *J. Opt.* **12**, 045703 (2010).
12. M. A. Ordal, R. J. Bell, R. W. Alexander, Jr., L. L. Long, and M. R. Querry, *Appl. Opt.* **24**, 4493 (1985).
13. M. G. Moharam and T. K. Gaylord, *J. Opt. Soc. Am.* **71**, 811 (1981).
14. W. Peng, L. Xi, X. Weng, X. Zhang, D. Zhao, and X. Zhang, *Chin. Opt. Lett.* **11**, 080604 (2013).
15. J. Wu, C. Zhou, H. Cao, A. Hu, W. Sun, and W. Jia, *Chin. Opt. Lett.* **11**, 060501 (2013).
16. C. J. Chang-Hasnain, Y. Zhou, M. C. Y. Huang, and C. Chase, *IEEE J. Sel. Top. Quantum Electron.* **15**, 869 (2009).
17. C. F. R. Mateus, M. C. Y. Huang, Y. F. Deng, A. R. Neureuther, and C. J. Chang-Hasnain, *IEEE Photon. Technol. Lett.* **16**, 518 (2004).